Available online on 15.11.2023 at http://jddtonline.info

Journal of Drug Delivery and Therapeutics

Open Access to Pharmaceutical and Medical Research

Open Access Full Text Article

Research Article

A comparative evaluation of two approaches for loading a therapeutic agent into custom fabricated electrospun nanofiber based innovative wound bandages

Tumelo H. Tabane*, and Bareki S. Batlokwa

Botswana International University of Science and Technology, College of Science, Department of Chemical and forensic sciences, Private Bag 16, Palapye, Botswana

Article Info:

Article History:

Received 18 Aug 2023
Reviewed 02 Oct 2023
Accepted 26 Oct 2023
Published 15 Nov 2023

Cite this article as:

Tabane TH, Batlokwa BS, A comparative evaluation of two approaches for loading a therapeutic agent into custom fabricated electrospun nanofiber based innovative wound bandages, Journal of Drug Delivery and Therapeutics. 2023; 13(11):73-80

DOI: http://dx.doi.org/10.22270/jddt.v13i11.6254

*Address for Correspondence:

Tumelo H. Tabane, Botswana International University of Science and Technology, College of Science, Department of Chemical and forensic sciences, Private Bag 16, Palapye, Botswana

Abstract

In this work, we evaluated two different approaches; the pvpi_blended and the pvpi_soaked approaches, of loading a model therapeutic agent, povidone-iodine (pvpi), into innovatively fabricated, electrospun poly-Ɛ-caprolactone (PCL) nanofiber based wound bandages. The two loading approaches were compared based on the critical parameters that an excellent wound dressing material must possess; loading capacity, therapeutic agent releasing behavior and wettability. From the results, the pvpi_blended approach PCL nanofiber mats with their higher calculated pvpi loading capacities of 97.0% outperformed the pvpi_soaked approach PCL nanofiber mats with 61.2%. They further outclassed the soaked_approach mats when it came to pvpi release time, recording a longer prolonged time of 98 min compared to shorter, faster time of 18 min for the release of 50% or more of pvpi for both. Furthermore, it was found out that the presence of the hydrophilic pvpi within the structure of the prepared PCL nanofiber mats bandages, altered the natural hydrophobicity of the pure PCL mats to slightly hydrophilic making them compatible with the hydrophilic wound exudates and their excellent absorbers. Additionally, the pvpi_loaded PCL nanofiber mat bandages exhibited favorable morphological attributes such as smooth surfaces, nano sized fibers with estimated diameters of 350 nm and high surface area to volume ratio, that supported high performance efficiency of the prepared materials. Overall, the blended presented itself as an approach of choice for incorporating medication when developing medicated nanofiber-based bandages such as the ones in this study, which are potential replacements of the conventional drug wasting, micro-structured cotton bandages.

Keywords: Electrospinning, Nanostructured bandages, Electrospun nanofiber bandages, Innovative drug delivery bandages, Smart bandages, Blended approach, Chronic wounds.

1. INTRODUCTION

Nanostructured materials such as electrospun nanofiber mats with large surface area to volume ratios and controllable morphologies, that can easily be functionalized, can be taken advantage of in chronic wound care management which is a challenge the world over, to produce the next generation wound dressing materials loaded with healing drugs that could give them smart drug delivery capabilities, thus providing cost effective wound care management solutions with improved therapeutic outcomes. Occurrence of injuries, that end up causing excruciating skin wounds to humans have led to the use of bandages for their care and management since time immemorial. The bandages are conventionally made from macro/micro structured materials such as linen or cotton, with fiber diameters above 1000 micrometers at molecular level [1,2,3], a feature which is making them not to enjoy all the advantages that come with nano size dimensions in modern nanotechnology. These materials have been found to be less cost effective, inefficient and pain-inducing due to their strong adherence to the wounds, thus, posing a burden to both the patients and health care systems during wound care management [4,5,6,7]. For example, currently, there is a lot of wastage of therapeutic agents or wound medicines which are usually smeared on the cotton bandages during wound dressing including when one replaces an old bandage with a new one during scheduled, periodical wound bandage change overs. In this case, the bandages play a passive role, of merely covering the wound area with very little therapeutic benefits offered from the smeared medicine which almost all of it is thrown away unused during bandage swapping. Despite all this, cotton bandages are still common and still largely employed at health facilities even to date. In order to reduce drug wastage and improve drug delivery as well as efficacy in wound care management, the advent of nanotechnology [8,9,10] has created the potential for the development of alternative wound dressing materials based on nano fibers which are nano structures that possess superior properties such as high surface area to volume ratios that could be favorable for high absorption of wound exudates as well as tunable functionalities that allow for the materials to be applied in different environments. For instance, these nanomaterials have opened avenues for the fabrication of newer, innovative wound care management dressing materials with potential to be equipped with effective drug loading, discharging and general healing properties in their structures. Nano fiber-based materials are well known for possessing unique, favorable traits such as controllable morphologies, large surface area to volume ratio and small pore sizes compared to

the conventional macro/micro-based materials [11,12]. Nano fibers have also been found to resemble extra cellular matrix, (ECM) [13,14,15] which is an integral layer within the human skin's structural composition, which in turn will further make the nano fiber based dressing materials better alternative dressing materials in terms of bio compatibility to the skin structure for accelerated wound healing and skin cell growth. Further to developing new and better materials for wound care management, there is equally a far greater need for more research to be geared towards efficient and smart drug delivery in this area. Thus, our endeavor in this regard, to develop, evaluate and compare two approaches for loading povidone iodine (pvpi) as a model therapeutic agent into the newly custom developed electrospun poly-Ɛ-caprolactone (PCL) [1617] nanofiber mats, as potential wound bandages with efficient drug delivery capabilities [18,19] in this work. Although known for poor degradability, PCL, a synthetic, aliphatic polymer has in the past been employed in clinical research for scaffold tissue engineering as it is easy to be functionalized, biocompatible, non-toxic and has been approved by the food and drug administration (FDA) center for use by humans [20,21,22]. Additionally, nano-fibrous PCL has been employed as a drug delivery vehicle owing to its mechanical properties that allow for drugs to be incorporated into it for their later release at targeted sites [23,24,25]. Even though, PCL is known to be hydrophobic in nature [26], as has been demonstrated in previous studies through contact angle measurements [27,28], it has proved to be easily modifiable especially if the drugs loaded in its matrix are hydrophilic, thus allowing the PCL matrix to be adjusted from hydrophobic (final measured contact angle of > 90°) to hydrophilic state (final measured contact angle of < 90°). Xia et al., has described this phenomenon when they developed novel composite tissue scaffold involving PCL. In their work, PCL scaffolds were found to have final measured contact angles of 112.9° (hydrophobic) whereas final measured contact angles of 87.4° - 79.5° (hydrophilic) were obtained after incorporating varying quantities of nano hydroxyapatite particles on the PCL scaffolds matrices. The results showed that the composite tissue scaffolds were made to have hydrophilic attributes due to the incorporation of the hydrophilic hydroxyapatite nano particles [29] which are the much needed traits for an excellent wound dressing material. For our work, in this article, similar hydrophilicity experiments were performed by introducing a hydrophilic therapeutic agent, pvpi into the prepared electrospun PCL nanofiber mat matrix. The hydrophilicity characteristic that our newly prepared nano fiber mats attained, was key as it qualified the prepared nano fiber mats as wound exudates absorbers. Experimentally, electrospinning [30,31,32,33,34], as a versatile approach for nanofiber material fabrication, was employed in our work to fabricate poly-Ɛ-caprolactone (PCL) polymer into nanofiber mats. Furthermore, incorporation of pvpi into the fabricated nanofiber mats was performed employing two different approaches; the pvpi_blended and the pvpi_soaked approaches, which were comparatively evaluated based on pvpi loading capacities, pvpi releasing behavior and contact angle for wettability studies. The motive behind comparing the pvpi_loaded PCL nanofiber mats (pvpi_blended approach and the pvpi_soaked approach PCL nanofiber mats) obtained from the two different loading approaches was to evaluate the most effective way of incorporating a drug or medicine or therapeutic agent such as pvpi employed as a model in this study into the matrices of fabricated electrospun nanofiber mats. The comparative evaluation of the two different nanofiber mats that resulted from the two approaches was carried out based on the efficiency of each mat to; maximally load the drug, release over 50% of the loaded drug over a reasonably prolonged in a controlled fashion, wettability as well as the ability to absorb wound exudates as measured by contact angles which are also related to the hydrophilicity and hydrophobicity of a material. Final measured contact angles of 90° and below are said to be hydrophilic and tend to favor wound exudates absorption [35,36,37] The newly prepared nanofiber mats were found to be water loving and as wound exudates are largely water based, the two (the newly prepared nanofiber mats and the wound exudates) were compatible. Based on the pvpi_blended approach outperforming the pvpi_soaked approach for all the evaluated parameters that were considered in this work, the blended approach presented itself as the best approach to employ for the efficient incorporation of functional materials such as drugs/medicine within the matrices of newly developed nanofiber mats.

2. MATERIALS, ANALYTICAL INSTRUMENTS AND METHODS

2.1 materials

Polycaprolactone (PCL, Average Mn 80 kDa), Polyvinylpyrrolidone-iodine complex (pvpi), phosphate buffered saline (PBS), Chloroform (CFM, 99% purity), and N, N-dimethylformamide (DMF, 99.5% purity) were purchased from Sigma-Aldrich (Johannesburg, South Africa). All other chemicals employed were of reagent grade.

2.2 Analytical Instruments employed for preparation and characterization of the electrospun PCL fiber mats

Spraybase electrospinning platform employed was supplied by Avectas (Maynooth, Ireland). Evolution 201 UV-Vis spectrophotometer, Drying oven (TTM-J4) and a Nicolet iS10 FTIR spectrophotometer employed, were all purchased from Thermo Fisher Scientific (Johannesburg, South Africa). A field emission scanning electron microscope (FE-SEM) JSM-7100F employed, was purchased from JEOL Ltd (Welwyn GardenCity, United Kingdom), Thermogravimetric analyzer (TGA/DSC 3+ star system) employed, was purchased from Mettler-Toledo (Columbus, OH, USA).

2.3 Preparation of electrospun PCL fiber mats loaded with pvpi employing two loading approaches

A modified electrospinning method [38] was employed in this work to produce electrospun PCL fiber mats under optimized electrospinning parameters of 10% spinnable polymer concentration, 11.58 kV voltage, 20 µl min^{-1} feeding rate and 20 cm needle tip to collector distance. Two loading approaches (the pvpi_blended and the pvpi_soaked approaches) were independently employed to load a model pvpi therapeutic drug into the electrospun PCL fiber mats under the optimized electrospinning conditions.

In the pvpi_blended approach, optimized quantities of PCL pellets were dissolved in 70:30 (v/v) CFM and DMF 10 ml mixture to prepare a 10% (w/v) PCL spinnable solution. Thereafter, optimized 5% (w/w) pvpi was added and the solution was stirred overnight at room temperature to produce a PCL_pvpi blended spinnable solution. The solution was then electrospun into what we referred to as the pvpi_blended approach PCL fiber mats that were formed on an aluminum foil collector. The pvpi_blended approach PCL fiber mats were dried in an oven at 40 °C, then stored in a desiccator overnight for further analysis.

For the pvpi_soaked approach, the same preparatory steps and the optimized quantities as in the blending approach were employed to produce the PCL fiber mats except that the pvpi was not added. The PCL fiber mats were then soaked overnight in a pvpi solution that was separately prepared by dissolving 5% (w/w) pvpi in phosphate buffered saline (PBS) solution. The soaking approach resulted in what we referred

to as pvpi_soaked PCL fiber mats that were stored in a desiccator overnight for further analysis.

2.4 Characterization

2.4.1 Characterization of electrospun PCL fiber mats employing SEM

A field emission scanning electron microscope (FESEM) was employed to evaluate the morphology of the electrospun PCL fiber mats and estimate the fiber diameters of the same mats. To perform this, round mat pieces of 5 mm radius which were cut from the electrospun PCL fiber mats were supported on 1 cm tall sample holders, then sputter coated with gold and inserted into the system for acquisition of SEM images.

2.4.2 Characterization of electrospun PCL fiber mats and pvpi employing FTIR

To ascertain the presence of pvpi within the structure of the electrospun PCL fiber mats, FTIR spectra of electrospun PCL fiber mats were recorded by FTIR spectrometer in the wavenumber range of 650-4000 cm^{-1}. The recorded FTIR spectra of the electrospun PCL fiber mats were compared to the spectra of pure pvpi through peak analysis.

2.4.3 Characterization of the electrospun PCL fiber mats and pvpi employing TGA

To qualify the formed electrospun PCL fiber mats as thermally stable under temperature-controlled conditions, TGA analysis was performed as follows; 5 mg of pvpi and electrospun PCL fiber mats with and without pvpi were placed in separate TGA sample holders then subjected to heat from 25 °C to 400 °C, at a rate of 10 °C min^{-1} under nitrogen gas stream within a monitored timed duration. TGA curves were obtained and compared to that of the pure pvpi.

2.5 Loading capacities of the electrospun PCL fiber mats from the pvpi_blended and the pvpi_soaked approaches

To evaluate the pvpi loading capacities of the fiber mats between the pvpi_blended and the pvpi_soaked approaches, UV-Visible spectrophotometer was employed to record the pvpi absorbances to obtain the actual pvpi quantities and encapsulation efficiencies which were used to compare the two approaches.

For the pvpi_blended approach, 10 mg of the pvpi_blended PCL fiber mats were dissolved in 2 ml of 70:30 (v/v) mixture of CFM and DMF in reaction vials. The solutions were stirred for 15 min and their absorbances were measured in triplicates at an optimal λmax = 364 nm to determine the loaded pvpi quantities. These quantities were employed to calculate the pvpi loading capacities in percentages employing equation **1**, and encapsulation efficiencies (EE%) employing equation **2.** The values were then captured in a table. The same steps as described for the pvpi_blended approach were followed to obtain the pvpi loading capacities and encapsulation efficiencies for the pvpi_soaked approach.

Eq 1

$$pvpi\ loading\ (\%) = \frac{Meaured\ pvpi\ \ quantity\ (mg)}{mass\ of\ the\ loaded\ mat\ (mg)} x\ 100$$

Eq 2

$$EE\ (\%) = \frac{Measured\ pvpi\ \ quantity\ (mg)}{theoretical\ pvpi\ quantity\ (mg)} x\ 100$$

2.6 pvpi releasing behavior of the electrospun PCL fiber mats from the pvpi_blended and the pvpi_soaked approaches

A UV-Visible spectrophotometer was employed in this experiment to record pvpi absorbances at 20 min time intervals to obtain cumulative pvpi quantities for the comparison of the pvpi releasing behavior between the two approaches. To assess the pvpi releasing behavior for the pvpi_blended approach, 10 mg of pvpi_blended PCL fiber mats were incubated at 37 °C in 5 ml PBS solution in reaction vials. At 20 min intervals, 2 ml portions were withdrawn from the incubated solution and subsequently replaced with an equal withdrawn volume of fresh PBS solution. The absorbances of the withdrawn solutions were recorded in triplicates at an optimal λmax = 364 nm. This was repeated until there was a constant trend in the recorded absorbances. The absorbances were employed to calculate the quantities of pvpi released at each time interval. These quantities were then employed to determine the cumulative pvpi quantities in percentages via equation **3**. The pvpi releasing behavior for the pvpi_soaked approach was attained in the same manner as it was described for the pvpi_blended approach and the corresponding comparative line plots of cumulative pvpi release (%) against release time, for the two approaches were constructed. A 50% cumulative pvpi release (%) or more by the prepared materials was described as good enough. The approach with the highest prolonged release was marked by a longer release time. The corresponding release times for a particular common cumulative pvpi release (%) of 50% or more, described as good enough, for both approaches were noted and compared. Materials that exhibit prolonged (longer times) for cumulative pvpi releases (%) of 50% or more are the preferred materials when it comes to wound care management.

Eq 3

$$pvpi\ release\ (\%) = \frac{Cum\ pvpi\ quantity\ (mg)}{initial\ pvpi\ loaded\ (mg)} x\ 100$$

2.7 Contact angle measurements for wettability Studies on the electrospun PCL fiber mats

The wettability of the pvpi_loaded PCL fiber mats that exhibited excellent performance on both the pvpi loading and releasing experiments was studied through contact angle measurements. Typically, 1 x 1 cm^2 mats were cut and placed on glass slides on a flat surface. One drop of PBS solution was carefully placed on the mat surfaces. Absorption of PBS drop on the PCL fiber mat surfaces was monitored, with a snapshot image of the drop obtained once the drop was placed on the mat surfaces and another snapshot obtained after some time when almost all the drop was absorbed. This was performed in triplicates and the images were uploaded into the image J software which assisted in calculating the initial and final measured contact angles. The average initial and final measured contact angles were recorded.

2.8 Application of pvpi release data on Higuchi kinetic model

Usually a drug diffusion mechanism based on Higuchi kinetic model[39,40] is employed to study the cumulative invitro drug release of drug delivery systems involving water soluble drugs[41,42,43]. Since the pvpi used in this work is a water-soluble drug, the release data in this work was fitted to the Higuchi kinetic model (**Eq 4**) to understand the pvpi release kinetics and mechanisms from the electrospun PCL fiber mats. It must be noted that only the pvpi release data from the pvpi_loaded PCL fiber mats that exhibited best performance on both the pvpi loading and releasing experiments was the one whose data was evaluated. A plot corresponding to the pvpi release data against time was constructed based on the model equation **4** and corresponding correlation coefficient value (R^2) was determined. Only a linear plot with R^2 value of at least 0.900 confirmed that the pvpi release data fitted the Higuchi kinetic model

Eq 4, Higuchi model

$$Q = K_H \sqrt{t}$$

Where, Q is the cumulative quantity of pvpi released in time t, and K_H is the Higuchi release constant. The cumulative pvpi percentage releases were plotted against square root of time in minutes.

3 RESULTS AND DISCUSSION

3.1 The Prepared pvpi_blended and pvpi_soaked approach PCL fiber mats

Thin sheet-like-mats were obtained on the aluminum collector upon electrospinning. The sheet-like-mats were carefully harvested from the collector and stored for further analysis. From the pvpi_blended approach, the obtained sheet-like-mats were pale yellow. The pale-yellow color was homogeneous throughout the mat structure indicating the successful, uniform distribution of the loaded pvpi molecules throughout the surface structure of the obtained mats.

As for the pvpi_soaked approach, white sheet-like-mats were obtained at first, which only turned pale yellow after soaking them in the pvpi solution for an optimized time. The color appeared like pale yellow stains on the surface of the soaked mats indicating an uneven distribution of the pvpi molecules within the structure of the obtained mats.

3.2 Characterization results for the electrospun PCL fiber mats

SEM images, FTIR spectra and TGA curves for the pvpi_blended and the pvpi_soaked PCL fiber mats obtained did not show any notable difference, hence only the characterization results of the pvpi_blended PCL fiber mats were reported.

3.2.1 SEM images of the electrospun PCL fiber mats

From the SEM image in figure **1**, it was observed that randomly aligned long smooth fibers with no beads were formed. Employing the image J software, calculated fiber diameters from the SEM image gave an estimated average diameter of about 350 nm as per the fiber diameter distribution illustrated by the histogram in figure **2**. The fiber magnitude of 350 nm confirmed that the obtained electrospun PCL fiber mats were in the nano scale, hence, were nanofibers.

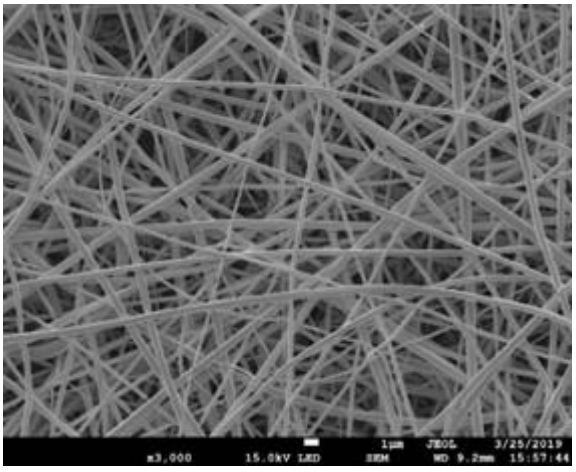

Figure 1 Scanning electron microscope image of pvpi_blended approach PCL fiber mats

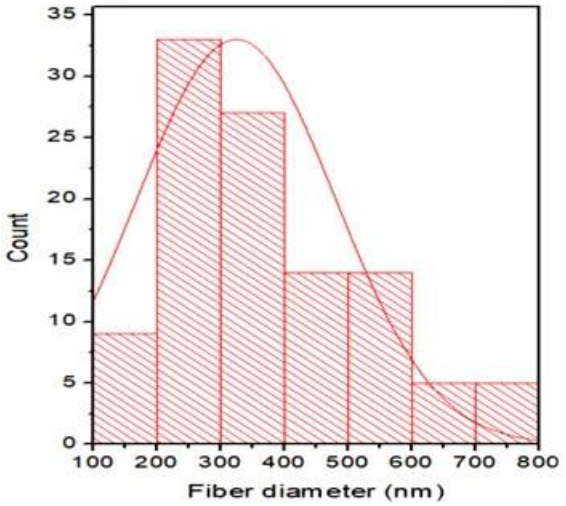

Figure 2 Estimated fiber diameter and distribution of the prepared pvpi_blended approach PCL fiber mats as calculated by the image J software from the SEM image in figure 1

3.2.2 FTIR spectra of pure pvpi, pure PCL nanofiber mats and pvpi_blended approach PCL nanofiber mats

From figure **3**, it was observed that almost all the peaks found in the spectrum of the pvpi_blended approach PCL nanofiber mats were identifiable either in the spectrum of pure pvpi or pure PCL nanofiber mats or in the spectra of both as expected, since the pvpi_blended approach PCL nanofiber mats were formed by combining the two, pure PCL and the pure pvpi. Of particular interest is a notable peak at 1700 cm^{-1} present in the spectra of pure pvpi as well as that of pvpi_blended approach PCL nanofiber mats and not the pure PCL nanofiber mats. Thus, it was concluded that the 1700 cm^{-1} indicated the presence of pvpi since the peak appeared only in the material containing pvpi in their structure. The 1700 cm^{-1} peak could be attributed to the amide functional group found in pyrrolidone ring of pvpi [44]. Other peaks of note were around 1650 cm^{-1} and 2950 cm^{-1} and could be attributed to the presence of -C=O and -CH groups, respectively on all the materials: pure PCL nanofiber mats, pvpi_blended approach PCL nanofiber mats and pure pvpi.

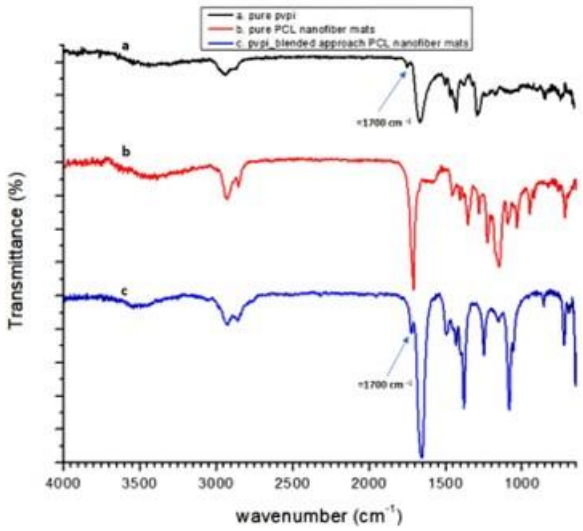

Figure 3 FTIR spectra of pure pvpi (a), pure PCL nanofiber mats (b) and pvpi_blended approach PCL nanofiber mats (c)

3.2.3 TGA curves of pure pvpi, pure PCL nanofiber mats and pvpi_blended approach PCL nanofiber mats

From the results shown in figure 4, it was observed that the TGA curves (**a** and **b**) for the pure PCL nanofiber mats and the pvpi_blended approach PCL nanofiber mats showed no mass loss change within the temperature range from 25 °C to about 300 °C, thus the materials were stable within the temperature range when compared to the TGA curve (**c**) of the pure pvpi that recorded a mass loss of about 15%, between 80 °C and 100 °C which was attributed to the water moisture content loss by evaporation and boiling processes respectively at those temperatures from the highly hygroscopic pvpi. The pure PCL nanofiber mats and the pvpi_blended approach PCL nanofiber mats experienced a huge mass loss change of over 80%, between 300 °C and 450 °C, as observed on the corresponding TGA curves on figure 4 (a) and (b) respectively. The loss was attributed to possible degradation and/or decomposition of the polymeric structure of the nanofiber mats into products such as carbon dioxide and volatile hexanoic acid as per literature [45] hence the two structures including the newly fabricated pvpi_blended approach PCL nanofiber mats were declared unstable at those temperatures, between 300 °C and 450 °C due to the mass loss.

3.3 Comparison of the pvpi loading capacities between the pvpi_blended approach and the pvpi_soaked approach PCL nanofiber mats

Initially, both the PCL nanofiber mats were subjected to a total of 5% (w/w) pvpi either through the pvpi_blended or the pvpi_soaked approach. From the results obtained, the pvpi_blended approach PCL nanofiber mats outclassed the pvpi_soaked approach PCL nanofiber mats as marked by pvpi actual loading capacity and encapsulation efficiency percentages of 4.85% out of 5.00% and 97.02%, respectively, which were higher than those of the pvpi_soaked approach PCL nanofiber mats with lower values at 3.06% out of 5.00% and 61.22% for pvpi actual loading capacity and encapsulation efficiency percentages, respectively, as displayed in table **1**. The higher values obtained for the pvpi_blended approach PCL nanofiber mats were attributed to the polymer-drug interaction during blending [46] which allowed the pvpi molecules to be evenly distributed over the large surface area of the nanosized fiber mats. On the other hand, the obtained lower values of pvpi loading capacity (3.06% out of 5.00%) and encapsulation efficiency (61.22%) for the pvpi_soaked approach PCL nanofiber mats were attributed to the uneven distribution of pvpi molecules within the structure of the PCL nanofiber mats as a result of the soaking approach that was employed.

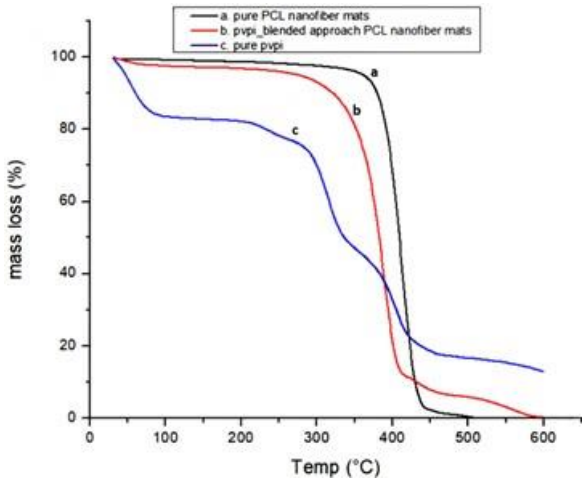

Figure 4 TGA curves of pure pvpi (c), pure PCL nanofiber mats (a) and pvpi_blended approach PCL nanofiber mats(b)

Table 1 Table showing pvpi loading capacities and encapsulation efficiencies for both the pvpi_blended and pvpi_soaked approach PCL nanofiber mats

pvpi_loaded PCL nanofiber mats	pvpi loading capacity (%) out of 5.00%	pvpi encapsulation efficiency (%)
pvpi_blended approach PCL nanofiber mats	4.85 ± 0.0056	97.02 ± 0.1063
pvpi_soaked approach PCL nanofiber mats	3.06 ± 0.0036	61.22 ± 0.0993

3.4 Comparison of the pvpi releasing behavior between the pvpi_blended approach and the pvpi_soaked approach PCL nanofiber mats

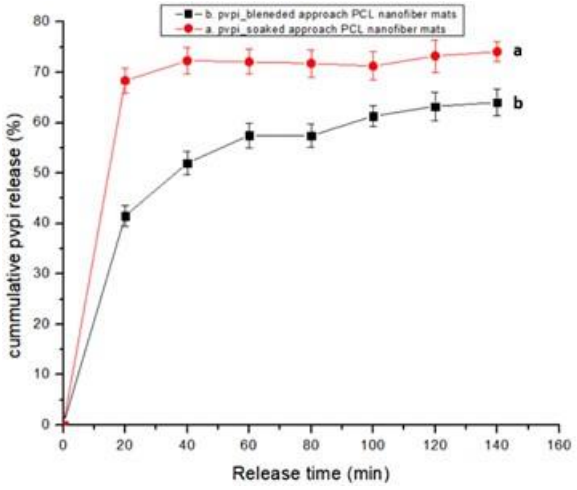

Figure 5 Pvpi release plots of the pvpi_blended (b) and pvpi_soaked approach PCL nanofiber mats (a)

From the results in figure 5, both the pvpi_blended approach PCL nanofiber mats, figure 5 (b) and the pvpi_soaked approach PCL nanofiber mats, figure **5** (a) released over 50% of pvpi within a reasonable time, thus exhibiting an excellent pvpi releasing behavior that cannot be attained by the conventional wound bandages as they struggle for at least 50% of the wound medicine that is usually smeared on them to be used up at the next bandage change over usually scheduled to next 3 to 5 days. Comparatively, the pvpi_blended approach PCL nanofiber mats attained a pvpi release of about 60% within a longer time of about 98 min compared to a short time of about 18 min taken by the pvpi_soaked approach PCL nanofiber mats to release the same comparable pvpi quantity as illustrated in figure **5**. This showed that the pvpi_blended approach PCL nanofiber mats exhibited the prolonged release for the drug to be used up, marked by the relatively longer pvpi releases, thus making it suitable for applications where prolonged drug releases are needed such as in wound care management, an area under study in this article. On the other hand, the pvpi_soaked approach PCL nanofiber mats with short pvpi release times of about 18 min for 60% pvpi release showed that it could be applicable to instances where the medicine is needed swiftly. Even though, the soaked approach recorded relatively poor prolonged releases, from figure **5** (**a**) it achieved higher maximum cumulative releases of about 70% which meant that 70% of the drug was accessible to be used up compared to about 60% of maximum cumulative releases by the blended approach, figure (**b**).

3.5 Measured contact angles for wettability studies on the pvpi_blended approach PCL nanofiber mats

From the contact angles results, the pvpi_blended approach PCL nanofiber mats initially displayed hydrophobic characteristics as marked by an initial average measured contact angle of 107° which changed almost after an hour to a final average measured contact angle of 89°. The change in contact angle from 107° to 89° was due to the presence of hydrophilic pvpi within the structure of the prepared PCL nanofiber mats, which altered the natural hydrophobicity of the PCL nanofiber mats, thus making the newly developed pvpi_blended approach PCL nanofiber mats slightly hydrophilic at 89°. From the literature, Razmshoar et al. [28] and Xia et al. [29] reported that pure PCL based nanofiber materials are naturally hydrophobic as per the contact angles measured at 97.86° and 112.98°, respectively. Generally, hydrophobic materials are characterized by contact angles above 90° whereas those showing hydrophilic behavior are characterized to have contact angles below 90° [47,36]. Final measured contact angles of 90° and below are said to be hydrophilic and tend to favor wound exudates absorption [35,36,37] The newly prepared nanofiber mats were found to have contact angles below 90°, (89°), thus hydrophilic (water loving) and as wound exudates are largely water based, the two (the newly prepared nanofiber mats and the wound exudates) were compatible.

3.6 pvpi release kinetics and mechanisms based on Higuchi model

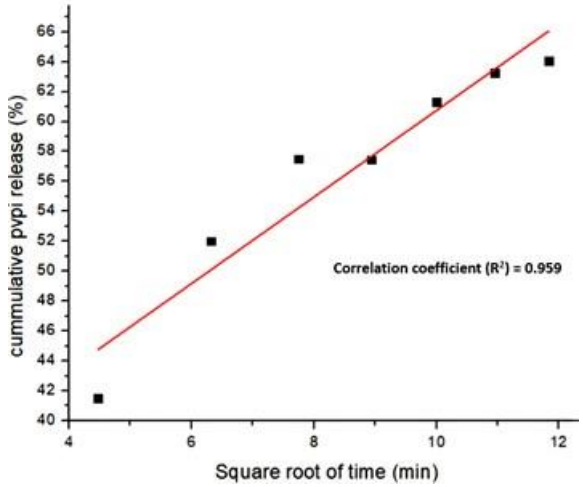

Figure 6 A linear plot representation of the pvpi release data fitted to the Higuchi kinetic model

In figure **6**, it was noted that the pvpi release kinetics for the pvpi_blended approach PCL nanofiber mats followed the Higuchi kinetic model in a linear fashion associated with a correlation coefficient (R^2) value of 0.959. The linear plot in figure **6**, together with the correlation coefficient (R^2) value of more than 0.900, R^2 = 0.959, confirmed that the diffusion mechanism of our pvpi release data by the pvpi blended approach nanofiber mats followed the Higuchi kinetic model. From literature, Monteiro et al. reported that the drug release kinetics based on the Higuchi model are described to be time-dependent fickian diffusion. This means that the quantity of the drug released decreased with time of exposure to the dissolution medium [48]. Moreover, Higuchi model supports the drug release kinetics that involve water soluble drugs such as pvpi in our case, and insoluble drug delivery vehicles, such as PCL nanofibers in this work, that do not significantly swell up upon contact with the releasing medium.

4. CONCLUSION

In conclusion, we comparatively evaluated two approaches of incorporating pvpi into custom-made electrospun poly-Ɛ-caprolactone (PCL) nanofiber mats with the potential to be applied as innovative medicated wound bandages. The two approaches that were employed were the pvpi_blended and the pvpi_soaked approaches which resulted in yellow coloured pvpi_blended approach PCL nanofiber mats and the pvpi_soaked approach PCL nanofiber mats, respectively. In comparison, the pvpi_blended approach PCL nanofiber mats significantly outperformed the pvpi_soaked approach PCL nanofiber mats when evaluating the results for both regarding pvpi loading capacity and the pvpi releasing behavior even though both mats showed similar, good, controlled releases of over 50% pvpi within a reasonable time. Furthermore, the pvpi_blended approach PCL nanofiber mats demonstrated a prolonged pvpi release as was marked by longer time periods taken to release 50% or more of the loaded pvpi compared to the pvpi_soaked approach PCL nanofiber mats which took a shorter time. The natural hydrophobicity of the PCL nanofiber

mats was also slightly altered by the presence of the hydrophilic pvpi within the structure of the prepared nanofiber mats, thus making the custom made pvpi loaded PCL nanofiber mats slightly hydrophilic and potentiating them as wound exudates absorbers. The custom-made PCL nanofiber mats were further found to possess excellent morphological attributes such as beadles, smooth and long nano-sized fibers as well as hydrophilic traits that supported their potential to function as wound exudates absorbers. Overall, the custom-made medicated electrospun nanofiber mats demonstrated remarkable qualities and emerged as promising alternatives that could replace the drug wasting conventional macro/micro structured cotton bandages in future. In our next work, we will employ the blended approach that outclassed the soaked approach in this article to fabricate uniformly medicated electrospun nanofiber mats that are dissolvable in wound exudates and would further improve drug delivery and efficacy whilst further reducing drug/medicine wastage when used as the next generation wound bandages.

Acknowledgement

Authors would like to thank the Botswana international university of science and technology (BIUST), through the Office of Research, Development, and Innovation (ORDI) for providing all the reagents, instruments and the platform to undertake the whole research reported in this paper.

Declaration of Competing Interest:

No competing interests were declared.

References

1. Pereira RF, Bártolo PJ. Traditional Therapies for Skin Wound Healing. Adv Wound Care. 2016;5(5):208-29. https://doi.org/10.1089/wound.2013.0506 PMid:27134765 PMCid:PMC4827280

2. Zahedi P, Rezaeian I, Ranaei-Siadat SO, Jafari SH, Supaphol P. A review on wound dressings with an emphasis on electrospun nanofibrous polymeric bandages. Polym Adv Technol. 2010;21(2):77-95. https://doi.org/10.1002/pat.1625

3. Selvaraj Dhivya VVP, Santhini E. Wound dressins- a review. 2015;5(July 2014):24-8. Available from: https://www.ncbi.nlm.nih.gov/pmc/articles/PMC4662938/ https://doi.org/10.7603/s40681-015-0022-9 PMid:26615539 PMCid:PMC4662938

4. Mogoşanu GD, Grumezescu AM. Natural and synthetic polymers for wounds and burns dressing. Int J Pharm. 2014;463(2):127-36. https://doi.org/10.1016/j.ijpharm.2013.12.015 PMid:24368109

5. Vincent Edwards J, Graves E, Prevost N, Condon B, Yager D, Dacorta J, et al. Development of a nonwoven hemostatic dressing based on unbleached cotton: A de novo design approach. Pharmaceutics. 2020;12(7):1-19. https://doi.org/10.3390/pharmaceutics12070609 PMid:32629845 PMCid:PMC7407894

6. Uzun M. A review of wound management materials. J Text Eng Fash Technol. 2018;4(1):53-9. https://doi.org/10.15406/jteft.2018.04.00121

7. Of EJ. European Journal of Orthodontics. Eur J Orthod. 1987;9(1):321-3. https://doi.org/10.1093/ejo/9.1.321

8. Hussain M, Wackerlig J, Lieberzeit PA. Biomimetic strategies for sensing biological species. Biosensors. 2013;3(1):89-107. https://doi.org/10.3390/bios3010089 PMid:25587400 PMCid:PMC4263596

9. Makaram P, Owens D, Aceros J. Trends in Nanomaterial-Based Non-Invasive Diabetes Sensing Technologies. Diagnostics. 2014;4(2):27-46. https://doi.org/10.3390/diagnostics4020027 PMid:26852676 PMCid:PMC4665544

10. Paul DR, Robeson LM. Polymer nanotechnology: Nanocomposites. Polymer (Guildf) [Internet]. 2008;49(15):3187-204. https://doi.org/10.1016/j.polymer.2008.04.017

11. Ahmadian A, Shafiee A, Aliahmad N, Agarwal M. Overview of Nano-Fiber Mats Fabrication via Electrospinning and Morphology Analysis. Textiles. 2021;1(2):206-26. https://doi.org/10.3390/textiles1020010

12. Ramakrishna S, Fujihara K, Teo WE, Yong T, Ma Z, Ramaseshan R. Electrospun nanofibers: Solving global issues. Mater Today [Internet]. 2006;9(3):40-50. https://doi.org/10.1016/S1369-7021(06)71389-X

13. Sell SA, Wolfe PS, Garg K, McCool JM, Rodriguez IA, Bowlin GL. The use of natural polymers in tissue engineering: A focus on electrospun extracellular matrix analogues. Polymers (Basel). 2010;2(4):522-53. https://doi.org/10.3390/polym2040522

14. Qing C. The molecular biology in wound healing & non-healing wound. Chinese Journal of Traumatology - English Edition. 2017. https://doi.org/10.1016/j.cjtee.2017.06.001 PMid:28712679 PMCid:PMC5555286

15. Chew S, Wen Y, Dzenis Y, Leong K. The Role of Electrospinning in the Emerging Field of Nanomedicine. Curr Pharm Des. 2006;12(36):4751-70. https://doi.org/10.2174/138161206779026326 PMid:17168776 PMCid:PMC2396225

16. Thomas R, Soumya KR, Mathew J, Radhakrishnan EK. Electrospun Polycaprolactone Membrane Incorporated with Biosynthesized Silver Nanoparticles as Effective Wound Dressing Material. Appl Biochem Biotechnol. 2015;176(8):2213-24. https://doi.org/10.1007/s12010-015-1709-9 PMid:26113218

17. Semnani D, Naghashzargar E, Hadjianfar M, Dehghan Manshadi F, Mohammadi S, Karbasi S, et al. Evaluation of PCL/chitosan electrospun nanofibers for liver tissue engineering. Int J Polym Mater Polym Biomater [Internet]. 2017;66(3):149-57. https://doi.org/10.1080/00914037.2016.1190931

18. Ponjavic M, Nikolic MS, Nikodinovic-Runic J, Ilic-Tomic T, Djonlagic J. Controlled drug release carriers based on PCL/PEO/PCL block copolymers. Int J Polym Mater Polym Biomater [Internet]. 2019;68(6):308-18. https://doi.org/10.1080/00914037.2018.1445631

19. Sadri M, Mohammadi A, Hosseini H. Drug release rate and kinetic investigation of composite polymeric nanofibers. Nanomedicine Res J. 2016;1(2):112-21.

20. Janmohammadi M, Nourbakhsh MS. Electrospun polycaprolactone scaffolds for tissue engineering: a review. Int J Polym Mater Polym Biomater [Internet]. 2019;68(9):527-39. https://doi.org/10.1080/00914037.2018.1466139

21. Ray PG, Pal P, Srivas PK, Basak P, Roy S, Dhara S. Surface modification of eggshell membrane with electrospun chitosan/polycaprolactone nanofibers for enhanced dermal wound healing. ACS Appl Bio Mater. 2018;1(4):985-98. https://doi.org/10.1021/acsabm.8b00169 PMid:34996140

22. Ferreira JL, Gomes S, Henriques C, Borges JP, Silva JC. Electrospinning polycaprolactone dissolved in glacial acetic acid: Fiber production, nonwoven characterization, and in Vitro evaluation. J Appl Polym Sci. 2014;131(22):37-9. https://doi.org/10.1002/app.41068

23. Baker SR, Banerjee S, Bonin K, Guthold M. Determining the mechanical properties of electrospun poly-ε-caprolactone (PCL) nanofibers using AFM and a novel fiber anchoring technique. Mater Sci Eng C. 2016; https://doi.org/10.1016/j.msec.2015.09.102 PMid:26652365

24. Mitxelena-Iribarren O, Riera-Pons M, Pereira S, Calero-Castro FJ, Castillo Tuñón JM, Padillo-Ruiz J, et al. Drug-loaded PCL electrospun nanofibers as anti-pancreatic cancer drug delivery systems. Polym Bull [Internet]. 2023;80(7):7763-78. https://doi.org/10.1007/s00289-022-04425-6

25. Semnani D, Nasari M, Fakhrali A. PCL nanofibers loaded with beta-carotene: a novel treatment for eczema. Polym Bull. 2018; https://doi.org/10.1007/s00289-017-2141-9

26. Archer E, Torretti M, Madbouly S. Biodegradable polycaprolactone (PCL) based polymer and composites. Physical Sciences Reviews. 2021. https://doi.org/10.1515/psr-2020-0074

27. Cho SJ, Jung SM, Kang M, Shin HS, Youk JH. Preparation of hydrophilic PCL nanofiber scaffolds via electrospinning of PCL/PVP-b-PCL block copolymers for enhanced cell biocompatibility. Polymer (Guildf) [Internet]. 2015;69(1):95-102. https://doi.org/10.1016/j.polymer.2015.05.037

28. Razmshoar P, Bahrami SH, Akbari S. Functional hydrophilic highly biodegradable PCL nanofibers through direct aminolysis of PAMAM dendrimer. Int J Polym Mater Polym Biomater [Internet]. 2020;69(16):1069-80. https://doi.org/10.1080/00914037.2019.1655751

29. Xia Y, Zhou PY, Cheng XS, Xie Y, Liang C, Li C, et al. Selective laser sintering fabrication of nano-hydroxyapatite/poly-ε-caprolactone scaffolds for bone tissue engineering applications. Int J Nanomedicine. 2013;8:4197-213. https://doi.org/10.2147/IJN.S50685 PMid:24204147 PMCid:PMC3818022

30. Ignatova M, Manolova N, Rashkov I. Electrospinning of poly(vinyl pyrrolidone)-iodine complex and poly(ethylene oxide)/poly(vinyl pyrrolidone)-iodine complex - a prospective route to antimicrobial wound dressing materials. Eur Polym J. 2007;43(5):1609-23. https://doi.org/10.1016/j.eurpolymj.2007.02.020

31. Sun K, Li ZH. Preparations, properties and applications of chitosan based nanofibers fabricated by electrospinning. Express Polym Lett. 2011;5(4):342-61. https://doi.org/10.3144/expresspolymlett.2011.34

32. Szentivanyi A, Chakradeo T, Zernetsch H, Glasmacher B. Electrospun cellular microenvironments: Understanding controlled release and scaffold structure. Adv Drug Deliv Rev [Internet]. 2011;63(4):209-20. https://doi.org/10.1016/j.addr.2010.12.002 PMid:21145932

33. Ekram B, Abdel-Hady BM, El-Kady AM, Amr SM, Waley AI, Guirguis OW. Optimum parameters for the production of nano-scale electrospun polycaprolactone to be used as a biomedical material. Adv Nat Sci Nanosci Nanotechnol. 2017;8(4). https://doi.org/10.1088/2043-6254/aa92b4

34. Schneider H, Steuber J, Du W, Mortazavi M, Bullock D. Polyethylene Oxide Nanofiber Production by Electrospinning. J Ark Acad Sci. 2016;70(1):211-5. https://doi.org/10.54119/jaas.2016.7027

35. Liu GS, Yan X, Yan FF, Chen FX, Hao LY, Chen SJ, et al. In Situ Electrospinning Iodine-Based Fibrous Meshes for Antibacterial Wound Dressing. Nanoscale Res Lett. 2018;13. https://doi.org/10.1186/s11671-018-2733-9 PMid:30284048 PMCid:PMC6170247

36. Huang FL, Wang QQ, Wei QF, Gao WD, Shou HY, Jiang SD. Dynamic wettability and contact angles of poly(vinylidene fluoride) nanofiber membranes grafted with acrylic acid. Express Polym Lett. 2010;4(9):551-8. https://doi.org/10.3144/expresspolymlett.2010.69

37. Morgado PI, Aguiar-Ricardo A, Correia IJ. Asymmetric membranes as ideal wound dressings: An overview on production methods, structure, properties and performance relationship. J Memb Sci [Internet]. 2015;490:139-51. https://doi.org/10.1016/j.memsci.2015.04.064

38. Eskitoros-Togay M, Bulbul YE, Tort S, Demirtaş Korkmaz F, Acartürk F, Dilsiz N. Fabrication of doxycycline-loaded electrospun PCL/PEO membranes for a potential drug delivery system. Int J Pharm. 2019;565(April):83-94. https://doi.org/10.1016/j.ijpharm.2019.04.073 PMid:31063838

39. Sciences H. Review kinetic modeling on drug release from controlled drug delivery systems. 2010;67(3):217-23.

40. Lamprecht A, Yamamoto H, Takeuchi H, Kawashima Y. A simple equation for description of solute release i. fickian and non-fickian release from non-swellable devices in the form of slabs, spheres, cylinders or discs Philip. J Control Release. 2003;90(3):313-22. https://doi.org/10.1016/S0168-3659(03)00195-0 PMid:12880698

41. Baishya H. Application of Mathematical Models in Drug Release Kinetics of Carbidopa and Levodopa ER Tablets. J Dev Drugs. 2017;06(02):1-8. https://doi.org/10.4172/2329-6631.1000171

42. Kumar P, Ganure AL, Subudhi BB, Shukla S. Design and comparative evaluation of in-vitro drug release, pharmacokinetics and gamma scintigraphic analysis of controlled release tablets using novel pH sensitive starch and modified starch-acrylate graft copolymer matrices. Iran J Pharm Res. 2015;14(3):677-91.

43. Paarakh MP, Jose PANI, Setty CM, Peter G V. Release Kinetics - Concepts and Applications. Int J Pharm Res Technol. 2019;8(1):12-20.

44. Pasteur L. Organic Chemistry I. A Hist Chem. 1964;749-800. https://doi.org/10.1007/978-1-349-00554-3_24

45. Su TT, Jiang H, Gong H. Thermal stabilities and the thermal degradation kinetics of poly(ε-caprolactone). Polym - Plast Technol Eng. 2008;47(4):398-403. https://doi.org/10.1080/03602550801897695

46. Ghasemiyeh P, Mohammadi-Samani S. Polymers Blending as Release Modulating Tool in Drug Delivery. Frontiers in Materials. 2021. https://doi.org/10.3389/fmats.2021.752813

47. Hadavi Moghadam B, Hasanzadeh M, Haghi AK. On the contact angle of electrospun polyacrylonitrile nanofiber mat. Bulg Chem Commun. 2013;45(2):169-77.

48. Monteiro MSSB, Lunz J, Sebastião PJ, Tavares MIB. Evaluation of Nevirapine Release Kinetics from Polycaprolactone Hybrids. Mater Sci Appl. 2016;07(11):680-701. https://doi.org/10.4236/msa.2016.711055